frontiers | Frontiers in Nanotechnology

TYPE Original Research
PUBLISHED 29 January 2026
DOI 10.3389/fnano.2026.1741495

OPEN ACCESS

EDITED BY
Yi Wang,
Eindhoven University of Technology,
Netherlands

REVIEWED BY
Yuncai Feng,
Qingdao University of Technology, China
Chao Dong,
Hewlett-Packard, United States

*CORRESPONDENCE
Zijian Zhang,
zzjian@hust.edu.cn

RECEIVED 07 November 2025
REVISED 22 December 2025
ACCEPTED 12 January 2026
PUBLISHED 29 January 2026

CITATION
Zhang Z (2026) Regularized topology optimization for light trapping structure in solar cells.
Front. Nanotechnol. 8:1741495.
doi: 10.3389/fnano.2026.1741495

Regularized topology optimization for light trapping structure in solar cells

Zijian Zhang*

School of Physics, Huazhong University of Science and Technology, Wuhan, China

Efficient light trapping bulk structures can significantly enhance light absorption in solar cells while reducing manufacturing costs. However, locating the optimal set of design parameters within a complex solution space remains challenging. Although numerous optimization algorithms have been employed to optimize bulk structure topologies, most treat the problem as purely mathematical, overlooking established physical principles such as light trapping and anti-reflection theories. By integrating both light-trapping and anti-reflection regularization, we obtain a 2 dimensional silicon inverted pyramid array (IPA) structure with an absorption rate of 0.7076, which yields a relative enhancement of 11.6% over the non-regularized baseline.

KEYWORDS

anti-reflect film, light trapping, optimization, physics-informed algorithms, regularization

1 Introduction

Light trapping structures are widely employed in solar cell research to enhance light absorption and reduce costs (Yablonovitch, 1982; Wang et al., 2014; Yu et al., 2011; Peter Amalathas and Alkaisi, 2019; Li et al., 2020; Massiot et al., 2020; Zhou and Biswas, 2008; Cao et al., 2021). Numerous designs, including inverted pyramid arrays (Yokogawa et al., 2017), triangular gratings (Dewan et al., 2009), nanoholes (Raman et al., 2011), nanowires (Garnett and Yang, 2010), nanocones (Wang et al., 2012), and photonic crystals (Bermel et al., 2007), have been proposed based on physical intuition. However, the complex nature of light-matter interactions makes it challenging to derive optimal structural parameters through intuition alone.

To address this, various optimization algorithms have been applied to optimize light trapping geometries (Campbell et al., 2019; Newton, 2007; Hestenes and Stiefel, 1952; Donald, 1963; Holland, 1992; Poli et al., 2007; Storn and Price, 1997; Rocca et al., 2011; Hansen et al., 2003). Kordrostami et al. used particle swarm optimization (PSO) to tune nanowire dimensions and inclination angles (Zoheir and Sheikholeslami, 2020), Wang et al. developed a genetic algorithm (GA)-based topology optimization framework (Wang et al., 2013), and Guo et al. designed broadband anti-reflection coatings through an ant colony algorithm (ACA) (Guo et al., 2014). While effective, these methods typically treat the optimization as a purely mathematical problem, neglecting established physical principles.

Regularization offers a way to incorporate such physical intuition by introducing a bias term into the objective function (Tian and Zhang, 2022; Benning and Burger, 2018; Kayri, 2016; Wen et al., 2018). In this work, we employ the covariance matrix adaptation evolution strategy (CMA-ES) (Auger et al., 2012) to optimize inverted pyramid arrays, integrating light trapping and anti-reflection theories into a regularization term. Our results demonstrate that each physical model individually enhances CMA-ES performance.

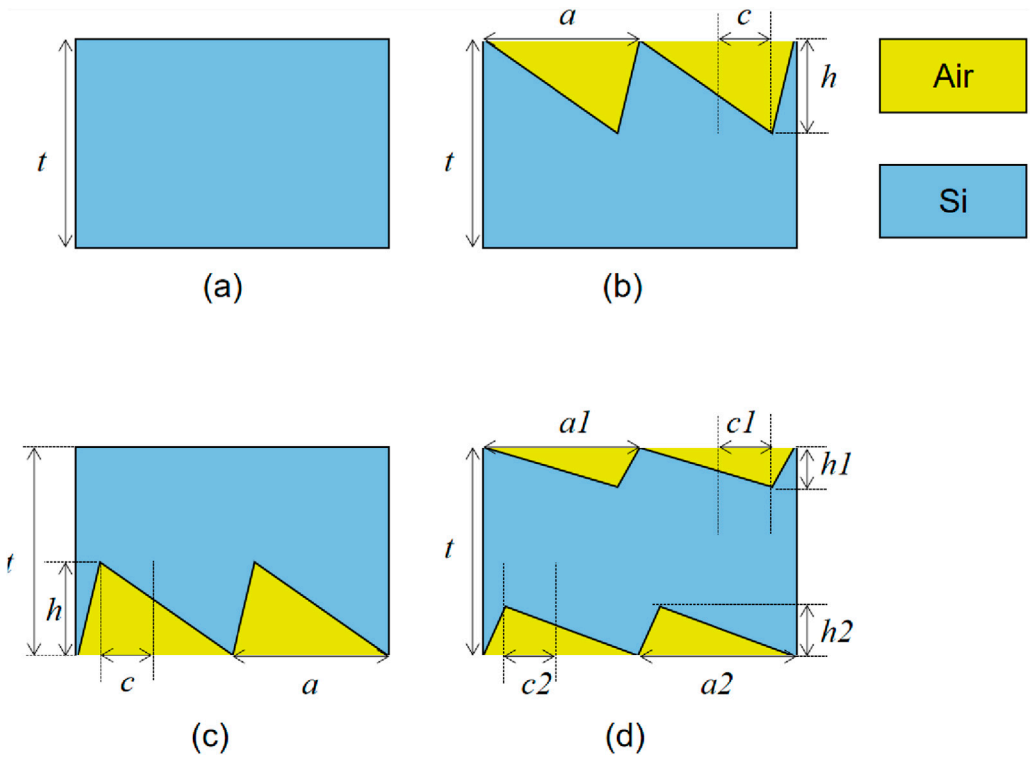

FIGURE 1
Two dimensional IPA structures in air. In all subplots, blue represent absorption layer which is filled with silicon, yellow represent IPAs which are filled with air. A mirror is placed at the bottom to enhance the absorption rate. The base, height and off-center distance of IPAs are denoted by *a*, *h*, and *c*, respectively. The thickness of the bulk structures is denoted by *t*. **(a)** The unpatterned bulk structure. **(b)** The top-only IPA structures. **(c)** The bottom-only IPA structures. **(d)** The double-sided IPA structures.

Moreover, combining both theories into a single regularization term yields greater improvement than either alone.

2 Methods

Figure 1 presents a schematic of the bulk structures with inverted pyramid arrays (IPAs). Incident light illuminates the structure vertically from above and is absorbed within the absorption layer. The structure comprises two regions: the blue area represents the silicon absorption material, while the yellow area denotes the IPA grating, which is modeled as air for simplicity. Inspired by double-sided grating designs (Wang et al., 2012), we investigate four configurations: (a) a top-only grating optimized with anti-reflection regularization; (b) a bottom-only grating optimized with light trapping regularization; (c) a double-sided grating optimized using both regularization terms. Key geometric parameters include the IPA length a, height h, absorption layer thickness t (consistent with (Cao et al., 2021)), and the off-center distance c, which breaks mirror symmetry and may enhance absorption limits (Yu et al., 2011). For the double-sided structure in (d), parameters $(a1, h1, c1)$ and $(a2, h2, c2)$ distinguish the top and bottom IPAs, with $a1 = a2$ due to periodicity constraints. The variables a, h, and c are optimized to maximize light absorption.

We use CMA-ES to optimize these IPA structures, and use the Average Absorption as the fitness function (i.e., the objective function of optimization algorithms). Average Absorption is used to quantify the light absorption of a bulk structure over a range of wavelengths. To introduce the quantitative definition of Average Absorption, we first define the light absorption for a single wavelength. Let $P_{into}(\lambda)$ and $P_{out}(\lambda)$ be the Poynting flux into and out of a bulk structure at wavelength λ, then

$$\text{Absorption}(\lambda) = \frac{P_{into}(\lambda) - P_{out}(\lambda)}{P_{into}(\lambda)} \tag{1}$$

Equation 1 defines the light absorption rate of the bulk structure for wavelength λ. Next, we consider a set of wavelengths $\Lambda = \{\lambda_1, \lambda_2, \ldots, \lambda_m\}$, then the Average Absorption is defined in Equation 2,

$$\text{Average Absorption}(\Lambda) = \frac{\sum_{\lambda \in \Lambda} \text{Absorption}(\lambda)}{m} \tag{2}$$

where Λ is the range of wavelength of interest. m is the total number of wavelengths in Λ. In our experiment, the wavelengths in Λ are sampled from 600 nm to 1,000 nm with a step size of 20 nm, resulting in $m = 21$ discrete points. This spectral range was selected based on the absorption characteristics of the IPA structures. As shown in Figure 2, most structures exhibited high and consistent absorption rates below 600 nm, with minimal variation across different designs. Conversely, between 1,000 nm and 1,100 nm, absorption performance was generally poor across all configurations. Consequently, the 600–1,000 nm window was

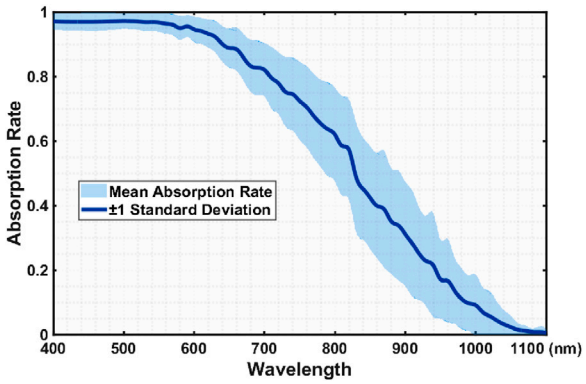

FIGURE 2
Average absorption spectrum and its statistical variability for 1,000 randomly sampled structures (Figure 1d) within the optimized parameter space. The horizontal axis represents the incident light wavelength (400–1,100 nm), and the vertical axis shows the corresponding absorption rate. The solid blue line indicates the mean absorption rate across all sampled structures. The light-blue shaded region denotes the range of ± 1 standard deviation, illustrating the dispersion in optical response resulting from structural variations under random parameter sampling.

chosen for optimization experiments, as it captures the region where structural differences lead to significant variations in absorption, thereby providing a meaningful basis for comparing the performance of different optimization algorithms.

The goal of light trapping optimization problems is to maximize the Average Absorption of the bulk structures with IPAs. a, h, and c are the design variables to be optimized. The constraints of the solution space are $0 < a < 2$ um, $0 < h < 2$ um and $0 < c < a/2$. Because the constraints of c depends on the value of a, to simplify, we define c'

$$c' = c \Big/ (a/2)$$

to be optimized, instead of c. The constraints of c' is $0 < c' < 1$ accordingly. Due to computational resource constraints, we focus on a two-dimensional scenario while aiming to retain three-dimensional generality. To achieve this, we perform simulations by uniformly extruding the two-dimensional structure into a three-dimensional setting along its longitudinal axis. This simplification, being equally applicable to all methods, ensures a fair comparison and does not invalidate our conclusions. The equivalent thickness of these structures is set to 2 um, which means all these structures share the same amount of silicon as the un-patterned film with $t' = 2$ um.

Regularization, a technique widely employed across disciplines such as mathematics, statistics, and computer science (Wen et al., 2018; Wang et al., 2020; Yun et al., 2019), can be implemented by introducing an additional term to the objective function of an optimization problem. For example, we can add a term $f(a, h, c)$ to the Average Absorption, and the Regularized Average Absorption RAA(a, h, c) can be defined in Equation 3.

$$\mathrm{RAA}(a, h, c) = \text{Average Absorption}(a, h, c) + f(a, h, c) \quad (3)$$

The optimization objective is thus redefined as maximizing the Regularized Average Absorption, which incorporates a physical prior $f(a, h, c)$ to guide the search. The influence of this prior, which can be derived from different theories, is tuned by a parameter α to balance the guidance and algorithmic flexibility (Equation 4).

$$\mathrm{RAA}(a, h, c) = \text{Average Absorption}(a, h, c) + \alpha \cdot f(a, h, c) \quad (4)$$

Let us now introduce the regularization term from light trapping theory. According to Yu's light trapping theory (Yu et al., 2011), the absorption coefficient A_T for a grating structure can be approximated by the expression given in Equation 7 of (Yu et al., 2011):

$$\mathrm{A_T} = \frac{2\pi\gamma_i}{\Delta\omega} \cdot \frac{M}{N}$$

where γ_i is the intrinsic loss rate of the resonance due to material absorption. M is the number of resonances in the frequency range $[\omega_0, \omega_0 + \Delta\omega]$, and N denotes the total number of plane-wave channels to which the structure can phase-match the resonance. Yu provides explicit expressions for M and N [Equations 13, Equation 15 in (Yu et al., 2011)]

$$\mathrm{M} = \frac{2n^2\pi\omega_0}{c^2}\left(\frac{L}{2\pi}\right)\left(\frac{d}{2\pi}\right)\Delta\omega$$

$$\mathrm{N} = 2\left\lfloor\frac{L}{\lambda}\right\rfloor + 1$$

where L is the period of the light trapping structure, t' is the thickness of the absorption layer, n is the refractive index of the material, λ is the wavelength of the incident light, and $\lfloor x \rfloor$ denotes the largest integer that is smaller than x. Therefore, the simplified expression for the absorption enhancement coefficient AT can be expressed as Equations 5, 6,

$$\mathrm{A_T} = Cons \cdot \frac{L}{2\left\lfloor\frac{L}{\lambda}\right\rfloor + 1} \quad (5)$$

$$Cons \equiv \frac{\gamma_i n^2 \omega_0 d}{c^2} \quad (6)$$

where *Cons* is held constant during our experiments. We notice that $\mathrm{A_T}$ depends on L and λ, therefore, the upper limit of absorption coefficient for a range of wavelengths can be expressed as Equation 7.

$$\mathrm{A_T}(L, \Lambda) = \frac{\sum_{\lambda\in\Lambda}\mathrm{A_T}(L, \lambda)}{m} \quad (7)$$

Since the period L is determined by the base length a of the tightly connected IPAs, we substitute a for L. By neglecting the constant term *Cons* (which is absorbed into the rescaled regularization strength α) and normalizing A_T to have a maximum value of 1, we obtain the relationship between the theoretical absorption coefficient A_T and the base length a in Figure 3.

We use A_T as the regularization term; therefore, the Regularized Average Absorption of light trapping theory (L-RAA) can be written as

$$\mathrm{L-RAA}(a, h, c) = \text{Average Absorption}(a, h, c) + \alpha \cdot \mathrm{A_T}(a) \quad (8)$$

Equation 8 encourages the optimization algorithms to search for values of a with a high value of A_T.

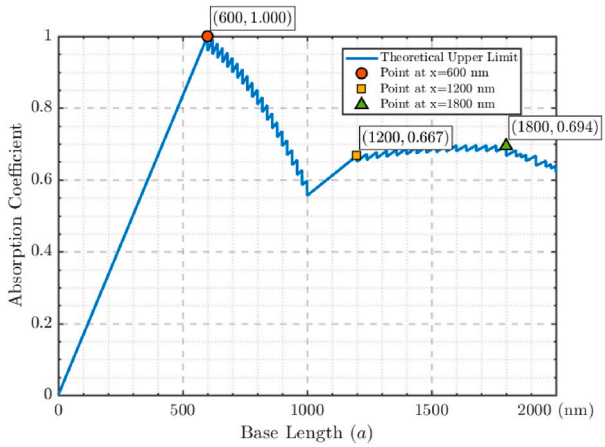

FIGURE 3
Theoretical upper limit of the absorption coefficient A_T as a function of base length a for IPAs. The blue curve shows the theoretical relationship, with key points at a = 600, 1,200, and 1800 nm highlighted by markers. The x-axis represents base length a, while the y-axis shows the relative absorption coefficient A_T.

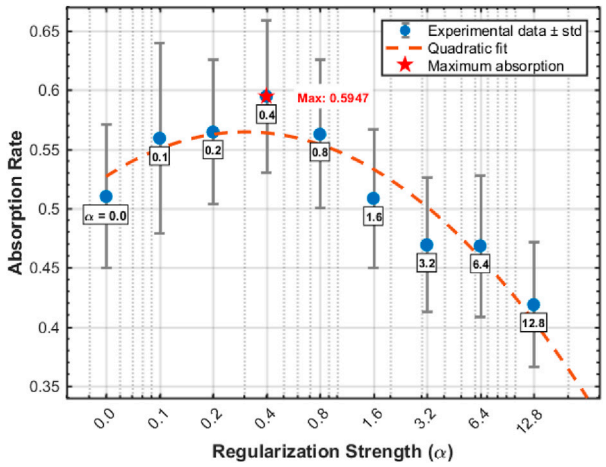

FIGURE 4
Average absorption rates obtained by the CMA-ES optimization algorithm for the bottom-only IPA structures under different regularization strengths. The blue scatter points represent the original data, while the red dashed line shows the fitted trend. The x-axis indicates the light trapping regularization strength (α), and the y-axis shows the average absorption of optimized bulk structures. The maximum absorption of 0.5947 occurs at α = 0.4 (highlighted in red), demonstrating the optimal regularization level for light trapping. The data points in the figure represent the average results obtained from 20 independent optimization trials for each regularization strength.

Let us now introduce the regularization term based on anti-reflection theory. A high aspect ratio, h/a, can provide a smooth refractive index transition from air to silicon, thereby enhancing light absorption. However, we notice that as a approaches zero, the term h/a diverges to infinity, which could destabilize the optimization algorithm. To avoid this singularity and to incorporate the physical scale of the structure, we modify the term to $h/(a+t')$, where t' represents the effective thickness of the optimized IPA structure. The Regularized Average Absorption of anti-reflection (A-RAA) can be written as Equation 9.

$$\mathrm{A-RAA}(a,h,c) = \mathrm{AverageAbsorption}(a,h,c) + \beta \cdot h/(a+t') \tag{9}$$

The CMA-ES algorithm was implemented with the following parameters. The initial shape parameters of the structure (a, h, c') were uniformly and randomly sampled within the defined parameter space: for a and h, the space ranged from 0 to 2000 nm with an initial step size of 500 nm; for c', the space ranged from −1 to 1 with an initial step size of 0.5. Additional algorithmic parameters included a convergence tolerance of 1×10^{-4}, a population size of 8, and a maximum of 60 iterations. To enforce the boundary constraints, any candidate solution with parameters sampled outside the prescribed ranges was discarded and replaced by a newly generated one.

S4 is a rigorous coupled-wave analysis (RCWA) method developed by Victor Liu (Liu and Fan, 2012). We use the Python version of S4 to simulate the light absorption of bulk structures. The simulations are performed under transverse magnetic (TM) polarized plane-wave incidence. The number of Fourier expansion orders (NumBasis) is set to 20, while all other simulation parameters retain their default values.

3 Results and analysis

Figure 4 plots the Average Absorption achieved by CMA-ES versus the regularization strength α (Equation 8) for a bottom-only grating structure. The results demonstrate that light trapping regularization provides a maximum relative boost of 16.5% compared to the unregularized case. As anticipated, Average Absorption first increases and then decreases with α. At low α, the objective function is dominated by the Average Absorption, and the regularization term serves as a mild guide, slightly improving search efficiency. However, when α becomes excessively large, the simplified physical prior—which does not fully capture the complex absorption physics—overwhelms the true objective. This misguides the optimization, causing performance to decline.

We note that the selection of the regularization strength (α) is crucial. In particular, when is too large, it can significantly degrade the algorithm's performance. Therefore, we adopt the following strategy: we start from a very small initial value (e.g., 0.00001), at which the maximum contribution of the regularization term remains below the numerical precision threshold of the optimization problem. Then we increase exponentially (e.g., by a factor of 2 each time) until the algorithm's performance is observed to improve first and then decline with increasing. The corresponding alpha at this transition is then approximately the optimal value. We employed the same strategy in the subsequent experiments.

For the top-only grating optimized using Equation 9, the Average Absorption shows a non-monotonic dependence on the anti-reflection regularization strength β (Figure 5). A maximum gain of 2.9% is achieved at an optimal β, beyond which the

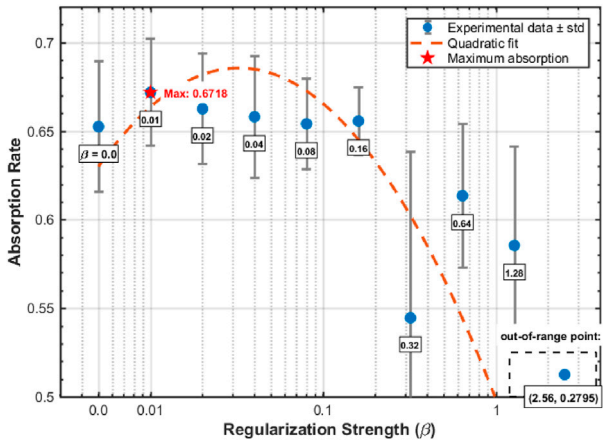

FIGURE 5
Average absorption rates obtained by the CMA-ES optimization algorithm for top-only IPA structures under different regularization strengths. The blue scatter points represent the original data, while the red dashed line shows the fitted trend. The x-axis indicates the anti-reflection regularization strength (β), and the y-axis shows the average absorption of optimized bulk structures. The maximum absorption of 0.6718 occurs at β = 0.01 (highlighted in red), demonstrating the optimal regularization level for anti-reflection. The data points in the figure represent the average results obtained from 20 independent optimization trials for each regularization strength.

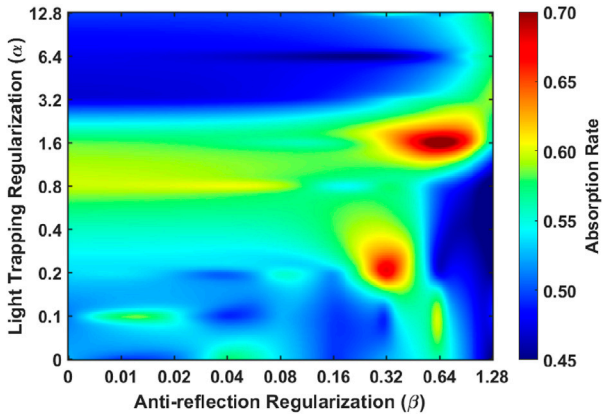

FIGURE 6
Optimization landscape of double-sided IPA structures using CMA-ES under varying regularization strengths. The heatmap visualizes the absorption rate across the two-dimensional regularization parameter space, where α (y-axis, log-scale) controls light trapping regularization and β (x-axis, log-scale) controls anti-reflection regularization. Color represents the optimized absorption performance. The maximum absorption of 0.7076 occurs at α = 1.6 and β = 0.64.

absorption rate falls. This pattern confirms that the relationship between absorption and regularization strength is general.

The light trapping regularization leads to a greater performance improvement than the anti-reflection approach. This advantage stems from their distinct theoretical foundations. The light trapping scheme is derived from a rigorous physical theory, which provides a precise analytical expression and a clear absorption upper limit. This strong theoretical foundation offers unambiguous guidance for the optimization process. In contrast, the anti-reflection regularization relies primarily on physical intuition.

Next, we integrated light trapping regularization with anti-reflection regularization Figure 6. The double-sided grating structure was optimized using the objective function defined in Equation 10,

$$\mathrm{D-RAA} = \text{Average Absorption} + \alpha \cdot A_T(a_1) + \beta \cdot h_2/(a_2 + d) \quad (10)$$

where α and β control the strength of anti-reflection and light trapping regularization, respectively. As shown in Figure 6, the maximum average absorption of 0.7076 is achieved when both α = 0.64 and β = 1.6. This configuration yields an 11.6% relative improvement compared to the non-regularized case, and surpasses the highest absorption rates obtained in the two previous single-regularization experiments.

To investigate the effect of regularization, we plotted two sets of violin plots to visualize the distribution of converged algorithm parameters, comparing the cases before and after applying light trapping and anti-reflection regularization, respectively. In Figure 7a, it can be observed that without regularization, the base length (a) of IPA structures predominantly converges around 1,600 nm, which corresponds to the broader region with smaller local maxima in Figure 3. In contrast, after applying regularization, the algorithm converges mostly at a = 600 nm, which aligns with the region exhibiting higher peak values in Figure 3. This clearly demonstrates that light trapping regularization effectively guides the algorithm to shift its convergence from a local maximum toward the global optimum. In Figure 7b, after applying regularization, the convergence region with small $h/(a+t')$ values disappears. Combined with the experimental result that regularization leads to higher absorption rates, this indicates that the primary role of regularization here is to prevent the algorithm from getting trapped in certain extreme regions, thereby improving its overall performance.

Figure 8 presents the optimized geometries and the corresponding electric field profiles obtained under four distinct regularization configurations. In Figure 8a, corresponding to the case without regularization ($\alpha = 0, \beta = 0$), the algorithm converges to a structure with a base length (a) = 1,492 nm and an aspect ratio (h/a) = 1.02. When only the light trapping regularization is applied (Figure 8b), the optimization yields a structure with (a = 600 nm) and (h/a = 0.94). Notably, this base length aligns with the theoretical maximum predicted at (a = 600, nm) in Figure 3. When only the anti-reflection regularization is applied (Figure 8c), The optimization yields a structure with (a = 634 nm) and a significantly larger aspect ratio (h/a = 3.32). Finally, for the double regularization case (Figure 8d), the algorithm converges to (a = 596 nm) and (h/a = 2.29). These results collectively demonstrate that different regularization schemes effectively guide the optimization algorithm towards distinct regions of the design space, each embodying a specific physical trade-off.

4 Discussion and conclusion

In conclusion, for the specific problem of optimizing the absorption rate of 2D silicon IPA structures, our results

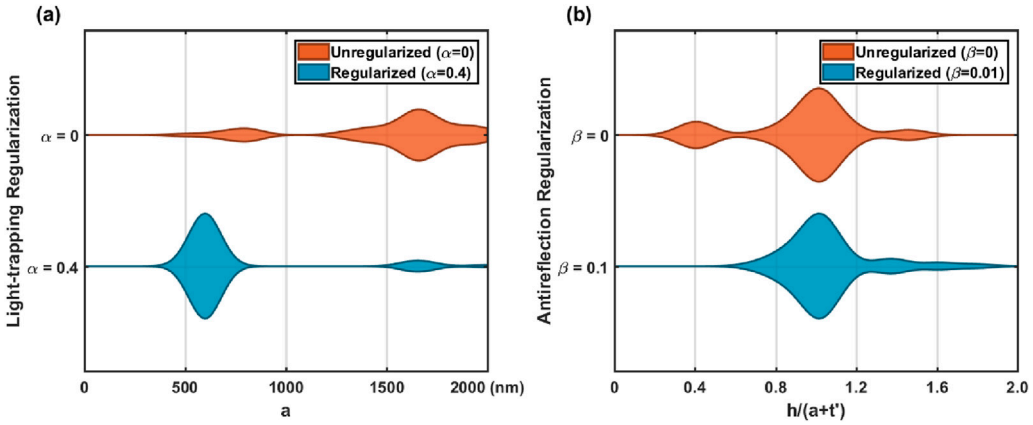

FIGURE 7
(a) Probability density distributions of base length *a* solutions optimized by CMA-ES under different regularization conditions. The orange and blue violin plots correspond to unregularized ($\alpha = 0$) and regularized ($\alpha = 0.4$) scenarios, respectively. **(b)** Probability density distributions of the approximate aspect ratio $h/(a + t')$ for solutions optimized by CMA-ES under different regularization conditions. The orange and blue violin plots correspond to unregularized ($\beta = 0$) and regularized ($\beta = 0.01$) scenarios, respectively.

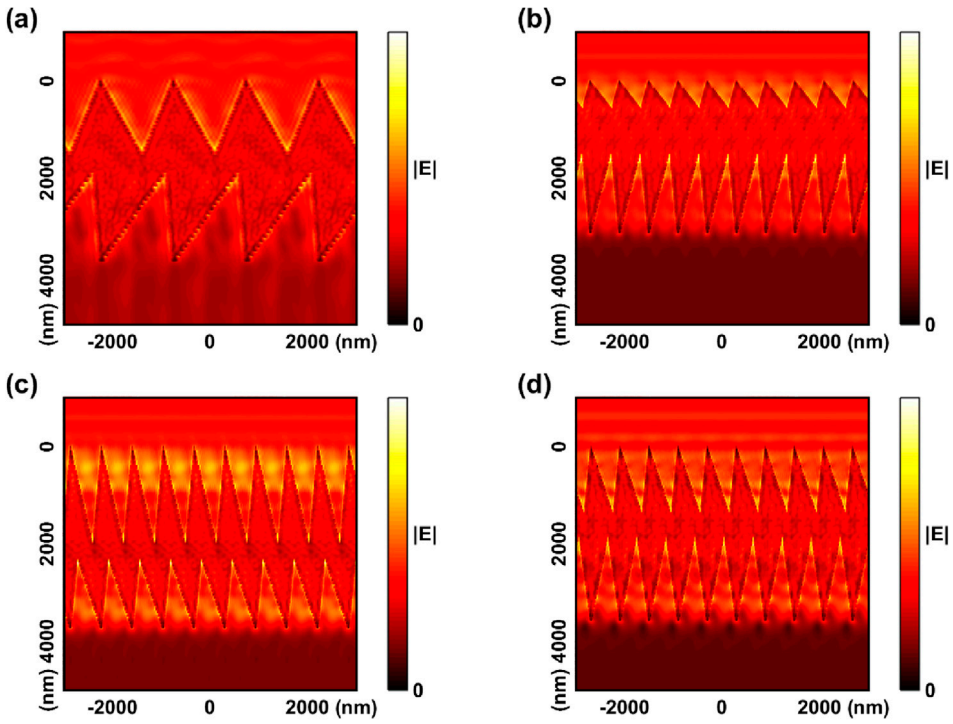

FIGURE 8
The optimized geometries and their corresponding electric field profiles for four distinct regularization configurations. Incident light enters from the top, is guided and absorbed within the structure, and is ultimately reflected back by a mirror positioned at the bottom. The color bar indicates the averaged electric field intensity over the incident spectrum. **(a)** Non-regularized structure ($\alpha = 0$, $\beta = 0$). **(b)** Light trapping regularized structure ($\alpha = 1.6$, $\beta = 0$). **(c)** Anti-reflection regularized structure ($\alpha = 0$, $\beta = 0.64$). **(d)** Double regularized structure ($\alpha = 1.6$, $\beta = 0.64$).

demonstrate that the performance of CMA-ES is influenced by the strength of the regularization term. Both light trapping and anti-reflection regularization were found to enhance its performance. This enhancement initially increases with regularization strength but diminishes beyond an optimal point, indicating a trade-off between guidance and over-constraint.

In recent years, topology optimization and inverse design based on adjoint/gradient methods have seen significant advancements (Kim et al., 2025; Pan and Pan, 2023; Mansouree et al., 2021). Our work demonstrates that regularization by physical priors offers a complementary path to improving photonic optimization. Instead of refining the

search strategy (how to optimize), we reformulate the problem itself (what to optimize). This reformulation—though tested with CMA-ES—is inherently transferable: by adding a regularization term, we superimpose a smooth, theory-driven gradient onto the often noisy fitness function. This provides consistent directional guidance in complex regions, which should facilitate convergence for both heuristic and gradient-based methods. However, this benefit is conditional. The regularization term directly alters the objective's gradient, meaning that an overly strong regularization term can dominate and mislead the search rather than guide it. To mitigate this risk, we introduced an adaptive scheme that starts with a minimal regularization weight and exponentially increases it to identify the optimal strength, thereby ensuring the prior provides constructive guidance. Consequently, regularization tends to be most effective when applied to complex problems with a well-defined physical prior. This is especially relevant for highly non-convex problems, where significant noise can make it challenging for algorithms to converge based solely on the problem's own gradient. In such scenarios, introducing an appropriate regularization term may help guide the iterative process toward a more desirable solution.

Data availability statement

The raw data supporting the conclusions of this article will be made available by the authors, without undue reservation.

Author contributions

ZZ: Writing – original draft, Writing – review and editing.

Funding

The author(s) declared that financial support was not received for this work and/or its publication.

Conflict of interest

The author(s) declared that this work was conducted in the absence of any commercial or financial relationships that could be construed as a potential conflict of interest.

Generative AI statement

The author(s) declared that generative AI was not used in the creation of this manuscript.

Any alternative text (alt text) provided alongside figures in this article has been generated by Frontiers with the support of artificial intelligence and reasonable efforts have been made to ensure accuracy, including review by the authors wherever possible. If you identify any issues, please contact us.

Publisher's note

References

Auger, A., and Hansen, N. (2012). "Tutorial cma-es: evolution strategies and covariance matrix adaptation," in *Proceedings of the 14th annual conference companion on Genetic and evolutionary computation*, 827–848.

Benning, M., and Burger, M. (2018). Modern regularization methods for inverse problems. *Acta Numer.* 27, 1–111. doi:10.1017/s0962492918000016

Bermel, P., Luo, C., Zeng, L., Kimerling, L. C., and Joannopoulos, J. D. (2007). Improving thin-film crystalline silicon solar cell efficiencies with Photonic crystals. *Opt. Express* 15 (25), 16986–17000. doi:10.1364/oe.15.016986

Campbell, S. D., Sell, D., Jenkins, R. P., Whiting, E. B., Fan, J. A., and Werner, D. H. (2019). Review of numerical optimization techniques for meta-device design. *Opt. Mater. Express* 9 (4), 1842–1863. doi:10.1364/ome.9.001842

Cao, Y., Zhang, Z., and Wang, K. X. (2021). Photon management with superlattice for image sensor pixels. *AIP Adv.* 11 (8), 085314. doi:10.1063/5.0058431

Dewan, R., Marinkovic, M., Noriega, R., Phadke, S., Salleo, A., and Knipp, D. (2009). Light trapping in thin-film silicon solar cells with submicron surface texture. *Opt. Express* 17 (25), 23058–23065. doi:10.1364/OE.17.023058

Donald, W. M. (1963). An algorithm for least-squares estimation of nonlinear parameters. *J. Soc. Industrial Appl. Math.* 11 (2), 431–441. doi:10.1137/0111030

Garnett, E., and Yang, P. (2010). Light trapping in silicon nanowire solar cells. *Nano Lett.* 10 (3), 1082–1087. doi:10.1021/nl100161z

Guo, X., Zhou, H. Y., Guo, S., Luan, X. X., Cui, W. K., Ma, Y. F., et al. (2014). Design of broadband omnidirectional antireflection coatings using ant colony algorithm. *Opt. Express* 22 (104), A1137–A1144. doi:10.1364/OE.22.0A1137

Hansen, N., Müller, S. D., and Koumoutsakos, P. (2003). Reducing the time complexity of the derandomized evolution strategy with covariance matrix adaptation (cma-es). *Evol. Comput.* 11 (1), 1–18. doi:10.1162/106365603321828970

Hestenes, M. R., and Stiefel, E. (1952). Methods of conjugate gradients for solving linear systems. *J. Res. Natl. Bureau Stand.* 49 (6), 409–436. doi:10.6028/jres.049.044

Holland, J. H. (1992). Genetic algorithms. *Sci. Am.* 267 (1), 66–73. doi:10.1038/scientificamerican0792-66

Kayri, M. (2016). Predictive abilities of bayesian regularization and levenberg–marquardt algorithms in artificial neural networks: a comparative empirical study on social data. *Math. Comput. Appl.* 21 (2), 20. doi:10.3390/mca21020020

Kim, J., Kim, J.-Y., Kim, J., Hyeong, Y., Neseli, B., You, J.-B., et al. (2025). Inverse design of nanophotonic devices enabled by optimization algorithms and deep learning: recent achievements and future prospects. *Nanophotonics* 14 (2), 121–151. doi:10.1515/nanoph-2024-0536

Li, K., Haque, S., Martins, A., Fortunato, E., Martins, R., Mendes, M. J., et al. (2020). Light trapping in solar cells: simple design rules to maximize absorption. *Optica* 7 (10), 1377–1384. doi:10.1364/optica.394885

Liu, V., and Fan, S. (2012). S4: a free electromagnetic solver for layered periodic structures. *Comput. Phys. Commun.* 183 (10), 2233–2244. doi:10.1016/j.cpc.2012.04.026

Mansouree, M., McClung, A., Samudrala, S., and Arbabi, A. (2021). Large-scale parametrized metasurface design using adjoint optimization. *Acs Photonics* 8 (2), 455–463. doi:10.1021/acsphotonics.0c01058

Massiot, I., Cattoni, A., and Collin, S. (2020). Progress and prospects for ultrathin solar cells. *Nat. Energy* 5 (12), 959–972. doi:10.1038/s41560-020-00714-4

Newton, I. (2007). The method of fluxions and infinite series: with its application to the geometry of curve-line:1736.

Pan, Z., and Pan, X. (2023). "Deep learning and adjoint method accelerated inverse design in photonics: a review," 10. *Photonics*, 852. doi:10.3390/photonics10070852

Peter Amalathas, A., and Alkaisi, M. M. (2019). Nanostructures for light trapping in thin film solar cells. *Micromachines* 10 (9), 619. doi:10.3390/mi10090619

Poli, R., Kennedy, J., and Blackwell, T. (2007). Particle swarm optimization. *Swarm Intell.* 1 (1), 33–57. doi:10.1007/s11721-007-0002-0

Raman, A., Yu, Z., and Fan, S. (2011). Dielectric nanostructures for broadband light trapping in organic solar cells. *Opt. Express* 19 (20), 19015–19026. doi:10.1364/OE.19.019015

Rocca, P., Oliveri, G., and Massa, A. (2011). Differential evolution as applied to electromagnetics. *IEEE Antennas Propag. Mag.* 53 (1), 38–49. doi:10.1109/map.2011.5773566

Storn, R., and Price, K. (1997). Differential evolution–a simple and efficient heuristic for global optimization over continuous spaces. *J. Glob. Optim.* 11, 341–359. doi:10.1023/a:1008202821328

Tian, Y., and Zhang, Y. (2022). A comprehensive survey on regularization strategies in machine learning. *Inf. Fusion* 80, 146–166. doi:10.1016/j.inffus.2021.11.005

Wang, K. X., Yu, Z., Liu, V., Cui, Yi, and Fan, S. (2012). Absorption enhancement in ultrathin crystalline silicon solar cells with antireflection and light-trapping nanocone gratings. *Nano Lett.* 12 (3), 1616–1619. doi:10.1021/nl204550q

Wang, C., Yu, S., Chen, W., and Sun, C. (2013). Highly efficient light-trapping structure design inspired by natural evolution. *Sci. Rep.* 3 (1), 1–8. doi:10.1038/srep01025

Wang, K. X., Yu, Z., Liu, V., Raman, A., Cui, Yi, and Fan, S. (2014). Light trapping in photonic crystals. *Energy and Environ. Sci.* 7 (8), 2725–2738. doi:10.1039/c4ee00839a

Wang, L., Huang, Y., Xie, Y., and Du, Y. (2020). A new regularization method for dynamic load identification. *Sci. Prog.* 103 (3), 0036850420931283. doi:10.1177/0036850420931283

Wen, F., Chu, L., Liu, P., and Qiu, R. C. (2018). A survey on nonconvex regularization-based sparse and low-rank recovery in signal processing, statistics, and machine learning. *IEEE Access* 6, 69883–69906. doi:10.1109/access.2018.2880454

Yablonovitch, E. (1982). Statistical ray optics. *J. Opt. Soc. Am.* 72 (7), 899–907. doi:10.1364/josa.72.000899

Yokogawa, S., Oshiyama, I., Ikeda, H., Ebiko, Y., Hirano, T., Saito, S., et al. (2017). IR sensitivity enhancement of CMOS image sensor with diffractive light trapping pixels. *Sci. Rep.* 7 (1), 1–9. doi:10.1038/s41598-017-04200-y

Yu, Z., Raman, A., and Fan, S. (2011). Nanophotonic light-trapping theory for solar cells. *Appl. Phys. A* 105 (2), 329–339. doi:10.1007/s00339-011-6617-4

Yun, S., Han, D., Oh, S. J., Chun, S., Choe, J., and Yoo, Y. (2019). "Cutmix: regularization strategy to train strong classifiers with localizable features," in *Proceedings of the IEEE/CVF international conference on computer vision*, 6023–6032.

Zhou, D., and Biswas, R. (2008). Photonic crystal enhanced light-trapping in thin film solar cells. *J. Appl. Phys.* 103 (9), 093102. doi:10.1063/1.2908212

Zoheir, K., and Sheikholeslami, H. (2020). Optimization of light trapping in square and hexagonal grid inclined silicon nanowire solar cells. *Opt. Commun.* 459, 124980.